

Novel indates $\text{Ln}_2\text{BaIn}_2\text{O}_7$, $n = 2$ members of the Ruddlesden–Popper family (Ln = La, Nd)

Maité Caldes, Claude Michel, Thierry Rouillon, Maryvonne Hervieu and Bernard Raveau

Laboratoire CRISMAT, UMR 6508 associée au CNRS, ISMRA, 6 Boulevard du Maréchal Juin, 14050 CAEN Cedex, France

Received 3rd October 2001, Accepted 11th December 2001
First published as an Advance Article on the web 30th January 2002

Stoichiometric $n = 2$ members of the Ruddlesden–Popper (RP) family have been synthesized. These oxides, $\text{Ln}_2\text{BaIn}_2\text{O}_7$ (Ln = La, Nd), crystallize in a tetragonal cell with $a = 5.9141(3)$ Å, $c = 20.8231(2)$ Å for La and $a = 5.8940(3)$ Å, $c = 20.467(1)$ Å for Nd. The crystal structure determination of the La oxide shows three remarkable structural features: (i) ordering of the La^{3+} and Ba^{2+} cations which sit in the rock salt and octahedral layers respectively; (ii) buckling of the octahedral layers; (iii) strong distortion of the rock salt layers forming an island like configuration. A comparison with the oxygen deficient $n = 2$ member $\text{Ba}_3\text{In}_2\text{O}_6$ is made.

Introduction

The ability of trivalent indium to adopt various coordinations—tetrahedral, octahedral, pyramidal—is an interesting feature for the generation of oxygen deficient perovskites and relatives. In the indates $\text{Sr}_2\text{In}_2\text{O}_5$ ¹ and $\text{Ba}_2\text{In}_2\text{O}_5$ ², the ordering of the oxygen vacancies leads to a brownmillerite structure, with alternating sheets of InO_6 octahedra and InO_4 tetrahedra. Several other indates derive from the Ruddlesden–Popper (RP) family $\text{Sr}_{n+1}\text{Ti}_n\text{O}_{3n+1}$.³ Their structures are built up from the intergrowth of one rock salt-type layer with perovskite slices, n octahedral layers thick, and the ordering of the oxygen vacancies create original structures. This is the case of the oxides $(\text{Ba}, \text{Sr})_3\text{In}_2\text{O}_6$ ^{4,5} which are isotypic to $\text{La}_2\text{SrCu}_2\text{O}_6$ ⁶ and derive from the $n = 2$ member, forming double pyramidal indium layers, intergrown with single rock salt layers. The indate $\text{Ba}_4\text{In}_2\text{O}_7$ ⁷ is also closely related to the RP family, since it derives from $\text{Ba}_3\text{In}_2\text{O}_6$ by introducing one additional BaO layer, between the pyramidal copper layers. The last example is shown by the indate $\text{Ba}_8\text{In}_6\text{O}_{17}$ ⁸ which represents the $n = 3$ member, built up of triple oxygen deficient perovskite layers intergrown with single ‘BaO’ layers.

The synthesis of stoichiometric indates in the RP series has curiously not been reported to date in spite of the ability of In^{3+} to adopt the octahedral coordination as in the perovskite LaInO_3 .⁹ We have thus explored this possibility substituting partly a trivalent lanthanide for barium. We report herein on the synthesis and crystal structure of the oxides $\text{Ln}_2\text{BaIn}_2\text{O}_7$ with Ln = La, Nd, $n = 2$ members of the RP series.

Experimental

$\text{Ln}_2\text{BaIn}_2\text{O}_7$ oxides were prepared by solid state reaction, starting from Ln_2O_3 (Ln = La, Nd and Eu), BaCO_3 and In_2O_3 in stoichiometric proportions. The mixtures were heated at 1300 °C for 12 h in air.

The samples were characterized by X Ray powder diffraction (XRPD) and electron microscopy. XRPD patterns were recorded with a Philips vertical goniometer, using $\text{CuK}\alpha$ radiation, in the range 5° – 100° , by step scanning with an increment of 0.02° (2θ). Cell parameters and crystal structure were refined using the profile refinement computer program Fullprof.¹⁰

Samples for electron microscopy were prepared by dispersing the crystallites in alcohol. The particles were deposited on a holey carbon film supported by a copper grid. The electron

diffraction (ED) study was carried out at room temperature (RT) using a JEOL 200CX electron microscope. The high resolution electron microscopy (HREM) was performed with a TOPCON 002B, operating at 200 KV (point resolution of 1.8 Å). HREM images calculations were carried out with the Mac-Tempas multislice program, varying the focus value and crystal thickness. The microscopes are equipped with energy dispersive spectroscopy (EDS) analyzers.

Results

For the conditions described above, a single phase is obtained for the compositions $\text{La}_2\text{BaIn}_2\text{O}_7$ and $\text{Nd}_2\text{BaIn}_2\text{O}_7$. By doping the lanthanum site by 0.2 Eu, an isotypic single phase is synthesized. The EDS analyses confirm the nominal cationic contents, namely La_2BaIn_2 , Nd_2BaIn_2 and $\text{La}_{1.8}\text{Eu}_{0.2}\text{BaIn}_2$. The reconstruction of the reciprocal space was carried out by tilting around the crystallographic axes. It evidences a tetragonal cell with $a \approx a_p\sqrt{2}$ and $c \approx 21$ Å, a_p referring to the parameter of the cubic perovskite cell. The [001], [010] and [110] ED patterns are given in Fig. 1. The reflection conditions are $h0l$: $h + l = 2n$, consistent with $P4_2nm$, $P4n2$ and $P4_2/mnm$ as possible space groups. On the basis of the ED results, the cell parameters were refined from the XRPD patterns (XRPD of $\text{La}_2\text{BaIn}_2\text{O}_7$ is shown in Fig. 2) to the following values:

$$\text{La}_2\text{BaIn}_2\text{O}_7: a = 5.9141(3) \text{ \AA} \text{ and } c = 20.831(2) \text{ \AA}$$

$$\text{Nd}_2\text{BaIn}_2\text{O}_7: a = 5.8940(3) \text{ \AA} \text{ and } c = 20.467(1) \text{ \AA}$$

$$\text{La}_{1.8}\text{Eu}_{0.2}\text{BaIn}_2\text{O}_7: a = 5.9188(3) \text{ \AA} \text{ and } c = 20.803(2) \text{ \AA}$$

The nature of the layer stacking along the c axis was determined by HREM, viewing the crystallites along the [110] direction. The overall HREM image recorded for $\text{La}_2\text{BaIn}_2\text{O}_7$ (Fig. 3a) shows the high regularity of the layer-stacking mode. An example of the enlarged image is given in Fig. 3b, where the zones of high electron density appear as dark dots. One observes three rows of dark dots correlated to the rock salt-type layers, namely $[\text{LaO}]_\infty$ and $[\text{BaO}]_\infty$; a double row of staggered dots, spaced by about 2.9 Å along c and one single row, sandwiched between two rows of gray dots correlated to the $[\text{InO}_2]_\infty$ layers. These images show that the structure is built up from the intergrowth of one rock salt-type layer

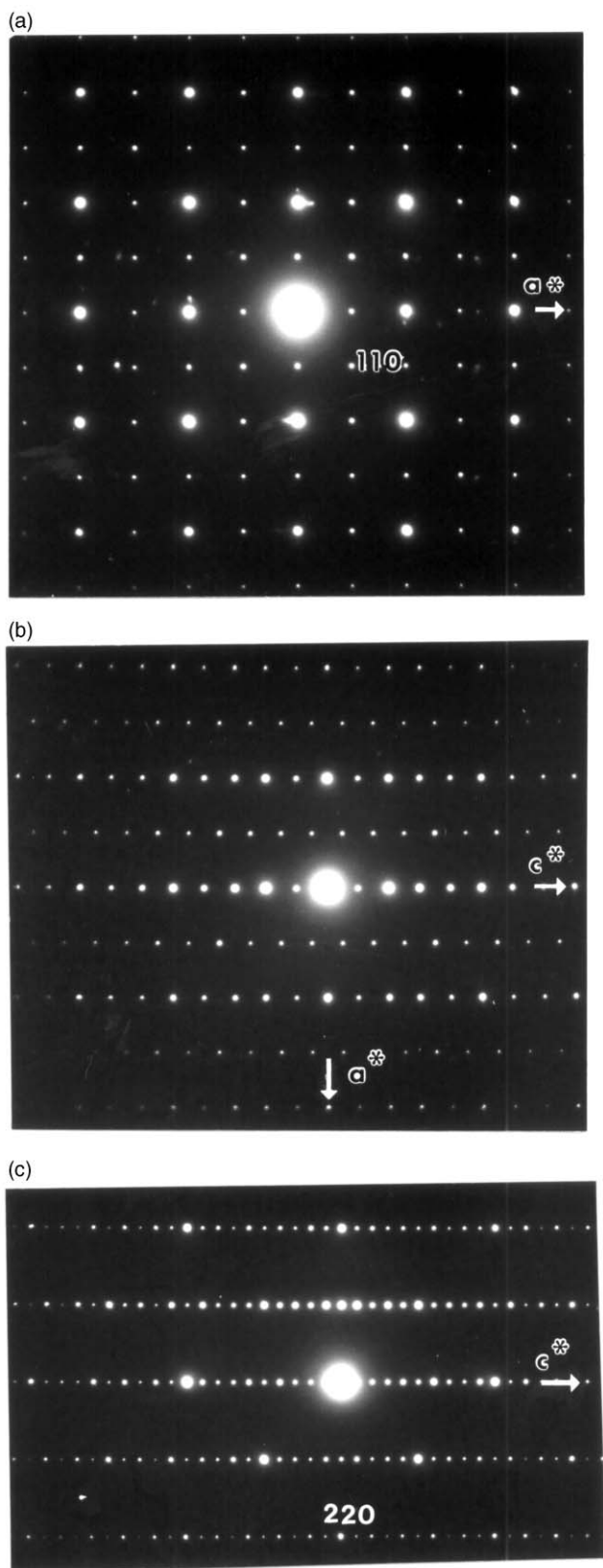


Fig. 1 a) [001], b) [010] and c) [110] ED patterns.

and a double perovskite layer, *i.e.* isotypic to $\text{Sr}_3\text{Ti}_2\text{O}_7^3$ and $\text{BaLa}_2\text{Fe}_2\text{O}_7$.¹¹ The simulated through focus series, calculated for different crystal thickness using the refined positional parameters (Table 1), fit perfectly with the experimental ones. The image calculated for a crystal thickness of 30 Å and a focus of -300 Å is inserted in Fig. 3b. The experimental through focus series exhibits a uniform and regular contrast, whatever the focus value.

A structure refinement was performed for $\text{La}_2\text{BaIn}_2\text{O}_7$ from

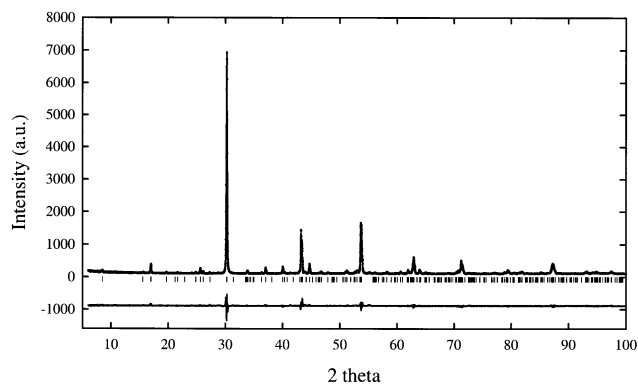


Fig. 2 X-Ray powder diffraction patterns of $\text{La}_2\text{BaIn}_2\text{O}_7$ ($\lambda = \text{CuK}\alpha$). At the bottom of the figure, the pattern is the difference between the experimental and the calculated one after refinement. Vertical bars show the Bragg angle positions.

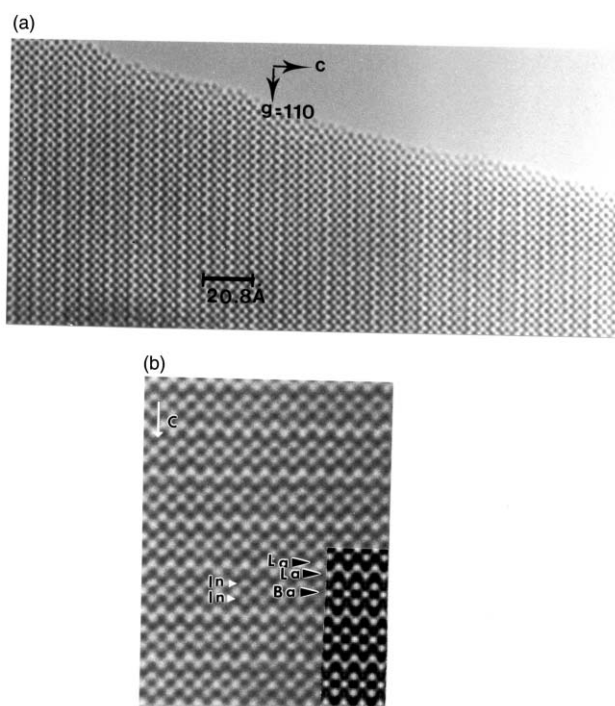


Fig. 3 [110] HREM images. a) overview showing the high regularity of the layer stacking mode along *c*. b) enlarged image: the cation positions appear as dark dots.

X ray powder data. Based on the electron microscopy results, calculations were carried out in the $P4_2/mnm$ space group. Although the scattering factors (for X ray and electron) of Ba^{2+} and La^{3+} are quite similar, we started from the positions

Table 1 Refined structural parameters from room temperature X ray diffraction data for $\text{BaLa}_2\text{In}_2\text{O}_7$. Space group $P4_2/mnm$, lattice constants $a = 5.9141(3)$ Å, $c = 20.831(2)$ Å, $Z = 4$, number of hkl : 231, $R_p = 0.121$, $R_{wp} = 0.182$, $R_B = 0.048$, $\chi^2 = 1.8$

Atom	Site	<i>x</i>	<i>y</i>	<i>z</i>	<i>B</i> /Å ²
Ba	4f	0.2580(6)	0.2580(6)	0.0	1.00(9)
La	8j	0.2711(3)	0.2711(3)	0.1842(1)	0.73(6)
In	8j	0.2580(4)	0.2580(4)	0.3944(1)	0.55(6)
O(1)	4g	0.789(5)	0.211(5)	0.0	1.3(4) ^a
O(2)	4f	0.186(3)	0.186(3)	0.296(1)	1.3(4) ^a
O(3)	4e	0.0	0.5	0.113(2)	1.3(4) ^a
O(4)	4e	0.0	0.0	0.131(2)	1.3(4) ^a
O(5)	4e	0.0	0.0	0.410(2)	1.3(4) ^a

^aConstrained to be refined with the same value.

given for $\text{BaLa}_2\text{Fe}_2\text{O}_7$.¹¹ *i.e.* considering that the lanthanum atoms sit in the rock salt (RS) layer (8j crystallographic sites) and barium in the perovskite (P) layer (4f sites) as shown in Fig. 4. A Bragg factor $R_B = 0.049$ is obtained for the positions given in Table 1.

These results demonstrate the possibility of stabilizing the stoichiometric $n = 2$ member of the RP family in the system La–Ba–In–O. $\text{La}_2\text{BaIn}_2\text{O}_7$, in spite of its close relationships with the oxygen deficient $n = 2$ member $\text{Ba}_3\text{In}_2\text{O}_6$, differs fundamentally from the latter by the distortion of its octahedral framework. The $[\text{InO}_2]_\infty$ layers parallel to (001) which form the InO_6 octahedra are strongly puckered in $\text{La}_2\text{BaIn}_2\text{O}_7$ due to the tilting of the octahedra (Fig. 4), whereas in contrast the $[\text{InO}_2]_\infty$ layers, which correspond to the basal planes of the pyramids in $\text{Ba}_3\text{In}_2\text{O}_6$ are planar. This tilting of the InO_6 octahedra implies a superstructure with respect to $\text{Ba}_3\text{In}_2\text{O}_6$: $a_{\text{La}_2\text{BaIn}_2\text{O}_7} \approx a_{\text{Ba}_3\text{In}_2\text{O}_6} \sqrt{2} \approx a_p \sqrt{2}$. It also explains the much smaller value of the c parameter of $\text{La}_2\text{BaIn}_2\text{O}_7$ (20.82 Å) compared to $\text{Ba}_3\text{In}_2\text{O}_6$ (21.70 Å), in spite of the presence of an additional layer of oxygen atoms.

The interatomic distances (Table 2) show that the InO_6 octahedra are almost regular, with In–O bonds ranging from 2.11 Å to 2.24 Å, similar to those observed in the InO_5 pyramids of $\text{Ba}_3\text{In}_2\text{O}_6$ (2.12–2.13 Å). Their geometry is thus very different from that of the InO_6 octahedra in the brownmillerite type structure of $\text{Ba}_2\text{In}_2\text{O}_5$, which are strongly distorted, with In–O distances ranging from 1.88 Å to 2.42 Å.

The second remarkable feature of this structure concerns the ordered distribution of La^{3+} and Ba^{2+} cations. The interatomic distances (Table 2) show indeed that the two sets of sites corresponding to the rock salt-type layers and to the perovskite cages of the octahedral layers, respectively, exhibit very different (La, Ba)–O bonds. Clearly, the rock salt layers exhibit shorter distances (mean value: 2.76 Å) than the perovskite cage (mean value: 3.08 Å) showing that they are preferentially occupied by lanthanum. Bond valence calculations¹² were also performed with Ba^{2+} and La^{3+} cations alternately located in the perovskite layer (4f sites) and in the rock salt layer (8j sites). For the 4f sites, the calculated valence V is +1.75 (Ba^{2+}) and +1.26 (La^{3+}) whereas for the 8j sites $V = +3.67$ (Ba^{2+}) and $V = +2.65$ (La^{3+}). These results confirm without ambiguity the location of Ba^{2+} in the perovskite cages and La^{3+} in the rock salt-type layers. As noticed above, this situation as already been observed in $\text{BaLa}_2\text{Fe}_2\text{O}_7$.¹¹

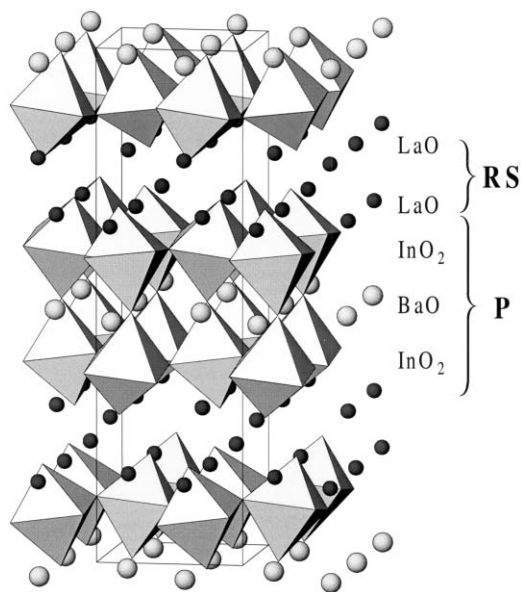


Fig. 4 Drawing of the structure of $\text{La}_2\text{BaIn}_2\text{O}_7$ showing the different layers forming the rock salt (RS) and perovskite (P) slabs respectively.

Table 2 Calculated interatomic distances

M–O	$d/\text{Å}$	M–O	$d/\text{Å}$
Ba–O(1)	$2.79(3) \times 2$	La–O(3)	$2.57(3) \times 2$
–O(1)	$3.15(3) \times 2$	–O(4)	$2.52(2) \times 1$
–O(3)	$3.15(3) \times 4$	–O(5)	$2.74(3) \times 1$
–O(4)	$3.48(3) \times 2$		
–O(5)	$2.76(3) \times 2$	In–O(3)	$2.11(1) \times 1$
		–O(3)	$2.24(2) \times 1$
La–O(2)	$2.43(2) \times 1$	–O(3)	$2.11(1) \times 2$
–O(2)	$2.50(2) \times 2$	–O(3)	$2.12(1) \times 1$
–O(2)	$3.49(2) \times 2$	–O(3)	$2.17(5) \times 1$

The last interesting characteristic of this structure deals with the large distortion of the barium and lanthanum polyhedra. The perovskite cages are indeed strongly distorted so that barium can be considered as having a ten-fold coordination instead of a twelve-fold one in the ideal perovskite, the two additional oxygen atoms (O(4)) sitting further at 3.48 Å. The rock salt-type layers are also strongly distorted, allowing the strains between the rock salt layers and the perovskite blocks to be released. The lanthanum cations and oxygen atoms are displaced from the ideal rock salt sites (Fig. 5) so that La^{3+} exhibits a seven fold (6 + 1) coordination (2.43 to 2.74 Å), two additional oxygens sitting much further away (3.49 Å). It results in an island-like atomic configuration of the rock salt layers which is closely connected to the tilting of the InO_6 octahedra of the adjacent octahedral layers. Such a configuration has been previously reported for other compounds such as $\text{SrTb}_2\text{Fe}_2\text{O}_7$ ¹¹ whose $\text{Sr}_3\text{Tl}_2\text{O}_7$ structure also exhibits distorted rock salt $[\text{TbO}]_\infty$ layers. This phenomenon is likely due to the size difference between the cations of the perovskite blocks (Ba^{2+} or Sr^{2+}) and of rock salt layers (La^{3+} or Tb^{3+}).

In conclusion, the oxides $\text{Ln}_2\text{BaIn}_2\text{O}_7$ ($\text{Ln} = \text{La}, \text{Nd}$) represent the only members ($n = 2$) of the stoichiometric RP indate family $\text{A}_n + 1\text{In}_n\text{O}_{3n + 1}$ that have been synthesized to date. The crystal chemistry of the lanthanum compound shows its great originality characterized by an ordering of the La^{3+} and Ba^{2+} cations in the form of layers. Such an ordering is closely connected to the buckling of the octahedral $[\text{In}_2\text{O}_6]_\infty$ layers and to the strong distortion of the $[\text{BaO}]_\infty$ layers. Further efforts will be made to understand the chemistry of the indium intergrowths and to explore their physical properties.

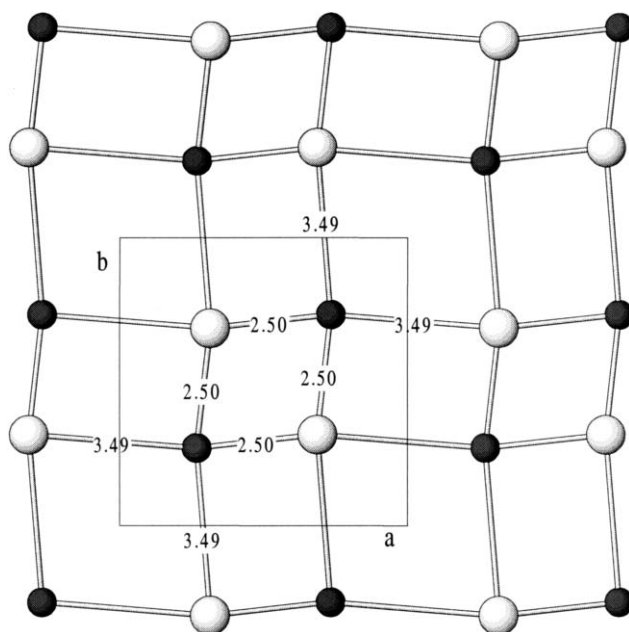


Fig. 5 LaO layer showing the two sets of La–O(2) distances and the island-like atomic configuration.

References

- 1 R. Von Schenck and Hk. Müller-Buschbaum, *Z. Anorg. Allg. Chem.*, 1973, **395**, 280.
- 2 D. H. Gregory and M. T. Weller, *J. Solid State Chem.*, 1993, **107**, 134.
- 3 S. N. Ruddlesden and P. Popper, *Acta Crystallogr.*, 1957, **10**, 538; S. N. Ruddlesden and P. Popper, *Acta Crystallogr.*, 1958, **11**, 54.
- 4 K. Mader and Hk. Müller-Buschbaum, *Z. Anorg. Allg. Chem.*, 1988, **559**, 89.
- 5 A. Lalla and Hk. Müller-Buschbaum, *Z. Anorg. Allg. Chem.*, 1990, **588**, 117.
- 6 N. Nguyen, L. Er-Rakho, C. Michel, J. Choynet and B. Raveau, *Mater. Res. Bull.*, 1980, **15**, 891.
- 7 A. Lalla and Hk. Müller-Buschbaum, *Z. Anorg. Allg. Chem.*, 1989, **573**, 12.
- 8 K. Mader and Hk. Müller-Buschbaum, *J. Less-Common Met.*, 1990, **157**, 71.
- 9 M. L. Keith and R. Roy, *Am. Mineral.*, 1954, **39**, 1.
- 10 J. R. Carvajal, *Collected Abstract of Powder Diffraction Meeting*, ed. J. Galy, Toulouse, France, 1990, p. 127.
- 11 D. Samaras, A. Collomb and J. C. Joubert, *J. Solid State Chem.*, 1973, **7**, 337.
- 12 N. E. Brese and M. O'Keeffe, *Acta Crystallogr., Sect. B*, 1991, **47**, 192.